

Adsorbate induced refacetting: Pb chains on Si(557)

This content has been downloaded from IOPscience. Please scroll down to see the full text.

2007 New J. Phys. 9 338

(<http://iopscience.iop.org/1367-2630/9/9/338>)

View [the table of contents for this issue](#), or go to the [journal homepage](#) for more

Download details:

IP Address: 194.95.157.145

This content was downloaded on 05/04/2017 at 13:05

Please note that [terms and conditions apply](#).

You may also be interested in:

[Vicinal surfaces for functional nanostructures](#)

Christoph Tegenkamp

[Adsorbate-induced nanostructuring of vicinal surfaces: the Ag–Cu system](#)

A

R Bachmann, F Ostendorf and S Speller

[One-dimensional collective excitations in Ag atomic wires grown on Si\(557\)](#)

U Krieg, C Brand, C Tegenkamp et al.

[Vicinal metal surfaces as nanotemplates for the growth of low-dimensional structures](#)

K Kuhnke and K Kern

[Adsorbate induced self-ordering of germanium nanoislands on Si\(113\)](#)

Thomas Schmidt, Torben Clausen, Jan Ingo Flege et al.

[Tailor-made ultrathin manganese oxide nanostripes: ‘magic widths’ on Pd\(1 1 N\) terraces](#)

C Franchini, F Li, S Surnev et al.

[Sheet plasmons in modulated graphene on Ir\(111\)](#)

T Langer, D F Förster, C Busse et al.

[Growth morphology of thin films on metallic and oxide surfaces](#)

Aleksander Krupski

[Scanning tunnelling microscopy of semiconductor surfaces](#)

H Neddermeyer

Adsorbate induced refacetting: Pb chains on Si(557)

M Czubanowski, A Schuster, S Akbari, H Pfnür
and C Tegenkamp¹

Institut für Festkörperphysik, Leibniz–Universität Hannover, Appelstrasse 2,
30167 Hannover, Germany

E-mail: tegenkamp@fkp.uni-hannover.de

New Journal of Physics **9** (2007) 338

Received 13 June 2007

Published 20 September 2007

Online at <http://www.njp.org/>

doi:10.1088/1367-2630/9/9/338

Abstract. The structure on the atomic and mesoscopic scale of Pb adsorbed on Si(557) has been investigated by high-resolution low energy electron diffraction (SPA-LEED). Depending on Pb coverage in the range between 1.2 and 1.6 monolayers (ML), formation of various facets [(112), (335), (223), and a meta-stable (557) orientation] is induced by the Pb layers. The facet orientation in general does not coincide with the macroscopic orientation of the (557) surface. After an initial annealing step to 600 K, starting with 1.2 ML of Pb, this new vicinality can be tuned gradually and reversibly even at temperatures below 180 K by further adsorption, but also by desorption of Pb. Superstructures of the Pb layers on the terraces were identified on the most stable (223) facets. Here parts of the devil's staircase and the stripe-incommensurate (SIC) phases known from Si(111) surfaces (Yakes *et al* 2004 *Phys. Rev. B* **69** 224103) develop. A new mechanism for facet formation with different orientations, based on avoidance of step decoration by adsorbed Pb, is proposed.

¹ Author to whom any correspondence should be addressed.

Contents

1. Introduction	2
2. Experimental set-up	3
3. Results	4
3.1. Clean Si(557) surface	4
3.2. Facet stabilization by a Pb monolayer	4
3.3. Devil's staircase phases	8
3.4. Coverage-dependent step trains	10
4. Discussion	13
5. Summary	15
References	15

1. Introduction

The growth of well-defined metallic overlayer structures on semiconductors has attracted much interest within the last few years. Low-doped semiconductor material is used in these cases, which acts as an effective insulator below room temperature. In the multilayer regime, these layers represent prototypes for the observation of quantum size effects (QSE), since they can be grown in some cases almost perfectly layer by layer with an atomically sharp interface [1]. Especially for metallic Pb layers, these quantum well states are responsible for the formation of 'magic' island heights [2]. Multiple changes of sign as a function of layer thickness in the Hall coefficient for Pb layers on Si(111) [3] turn out to be due to the thickness-dependent formation of the two-dimensional (2D) band structure, and are thus also related to the QSE.

Some of these systems can also be used to study (1D) structural and even electronic properties at concentrations below 1 monolayer (ML), which has recently opened a new field of study. However, instabilities are inherent in 1D systems and complicate the situation. The interplay between adsorbate and substrate interactions may allow to overcome part of these problems.

The 2D symmetry is either broken spontaneously as for In/Si(111) [4], e.g., and extremely anisotropic properties result from the combined lateral interactions between In and Si close to 1 ML. Alternatively, anisotropy is produced directly by use of a vicinal surface, and 1D metallic structures are generated far below monolayer concentration on each of the small terraces of the vicinal surface. An example is Au/Si(557), in which single Au chains on each small terrace are spontaneously formed at a concentration of only 0.2 ML. They exhibit the signature of almost 1D metallic bands in spectroscopy [5]. Using different vicinalities, e.g. (223), (335) and (557) the interaction between those metallic bands can be changed gradually [5, 6]. At these low concentrations only the local structure of the surface is rearranged, whereas the step-step distances do not or only weakly depend on coverage.

In this paper, we go to the other extreme, the situation of strongly coupled terraces in the coverage range around one physical monolayer and concentrate on structural aspects. With respect to the Si surface concentration of atoms, one physical monolayer corresponds to 1.33 ML on flat (111)-oriented Si surfaces. This assignment, neglecting the concentration adsorbed at step edges, will be used throughout this paper. As we show, the surface energy of the combined Pb/Si(557) system becomes strongly concentration dependent in the range between

1.2 and 1.4 ML, which leads to a Pb coverage-dependent refacetting of the whole surface to facet orientations that differ from the macroscopically given orientation.

This has important consequences also for the electronic properties of this surface. Recently, we have found that the formation of Pb chains on the Si(557) surface that is locally refaceted to a (223) orientation after adsorption of roughly one monolayer of Pb [7] (1.31 ML according to our calibration in this paper, see below) has quasi-1D properties of electrical conductance along these chains below a surface temperature of 80 K [8, 9]. Recent angle resolved photoemission spectroscopic (ARPES) measurements on these Pb monolayer chain structures demonstrate that at first glance the system electronically looks like an anisotropic, but 2D Fermi gas [10]. Conductance is obtained by Pb-modified surface bands that do not overlap with bulk Si bands so that pure surface conductance is observed [10]. Very close to the Fermi level, however, the periodicity of the Pb induced (223) facets normal to the steps plays a crucial role. It turns out that for this facet orientation the Fermi wavevector k_F in the direction normal to the steps corresponds exactly to half the reciprocal vector $g = 2\pi/d$ (d is the average step separation). Thus k_F coincides with the Brillouin zone boundary in this direction, which results in gap opening and nesting of the Fermi surface. As a result, no conductance can be found in this direction for the perfectly ordered facets. This new mechanism for 1D conductance is a result of 2D coupling between the individual terraces and the Pb-induced stabilization of a certain step-step separation. Thus not only the typical instabilities inherent to 1D systems are avoided. This system also demonstrates the intriguing possibilities to tailor surface structure by adsorbate concentration together with electronic properties.

Therefore, in order to elucidate these possibilities in more detail, we investigate hereby an analysis with high resolution low energy electron diffraction (SPA-LEED), how the interchain distance can be tuned gradually by varying Pb concentrations up to 1.6 ML starting at 1.2 ML. This includes step decoration, which occurs only at concentrations above 1.33 ML. For the Pb concentrations between 1.2 and 1.33 ML, the main field of investigation here, our results and the structural models are partly at variance with recently published suggestions, based on a much less complete data set [11].

2. Experimental set-up

The experiments were performed in an UHV chamber equipped with SPA-LEED and Auger spectroscopy. The base pressure was 1×10^{-9} Pa and better than 3×10^{-8} Pa during evaporation. Pb was evaporated out of a ceramic crucible heated by a tungsten filament. A microbalance was used to control the amount of Pb. The monolayer ($1 \text{ ML} = 7.84 \times 10^{14} \text{ atoms cm}^{-2}$) of Pb in this paper is given with respect to the Si(111) surface and the coverage was calibrated by LEED oscillations and thickness-dependent conductivity measurements. For the final calibration, we used the phase diagram for Pb/Si(111) measured in detail by Tringides and co-workers, see e.g. [12, 13]. In particular the DS-regime ('devil's staircase') was used to determine the coverage within 1% of a monolayer (for justification, see below). The Si(557) samples ($1 \times 1 \text{ cm}^2$) were mounted on a manipulator, which was cooled by ℓHe . Perfect Si(557) surfaces were prepared by degassing the sample for many hours until the pressure was below 1×10^{-8} Pa at 600°C . The removal of the oxide was done by heating the sample several times up to 1100°C . Higher flash temperatures rearrange the metastable (557) surface into large (111) domains separated by step bunches. The high-temperature steps were all performed by electron bombardment from the rear of the sample. For LEED and also for macroscopic transport measurements

a uniform phase distribution over the sample is of high importance, especially for Pb on Si substrates in the monolayer regime, as this paper demonstrates. Therefore, a uniform heating, i.e. temperature gradients of less than 5 K on the sample is necessary. This was achieved by a ring-shaped filament. The temperatures were measured pyrometrically and calibrated by Ni/NiCr thermocouples on dummy samples.

LEED measurements were typically done with a He-cooled sample close to 4 K, whereas adsorption and annealing was carried out at the temperatures indicated in the text.

3. Results

3.1. Clean Si(557) surface

Figure 1(a) shows the diffraction pattern within the first SBZ (surface Brillouin zone) of a clean Si(557) surface at an in-phase condition for the (00)-beam ($S = 5$, the scattering phases are given with respect to double steps of Si(111)). Besides the integer spots as marked, the miscut towards the $[\bar{1}\bar{1}2]$ direction reveals further signatures in the diffraction pattern: the integer spots are split along the mirror plane of the uniaxial surface (vertical direction). A (7×7) reconstruction with strongly elongated spots in $[\bar{1}\bar{1}2]$ direction characteristic for strongly anisotropic Si(111) terraces appears in between. In addition, streaks at 43% SBZ (corresponding to half the distance between the step train of integer order spots) along the $[1\bar{1}0]$ direction are visible, indicating period doubling along the step edges. Whereas the split (1×1) spots are fairly sharp, a signature of strong periodicity and correlation along the step train, little correlation between different terraces exists for the (7×7) structure. As we show below by comparison with STM, this is a direct consequence of the equilibrium structure of the Si(557) surface.

This LEED image is a consequence of the fact that the (557) surface is not homogeneously stepped [14] with respect to steps of single atomic height. The equilibrium structure of Si(557) consists of triple steps [15]. A homogeneous step density implies a nominal terrace width of $5\frac{2}{3}a_0$ (row distance $a_0 = 3.32 \text{ \AA}$) with a spot splitting of 21.3% SBZ, contrary to our observation. Instead, the surface consists of minifacets with (111) and (112) orientations, as seen in the STM picture shown in figure 1(c) and schematically modeled in figure 1(b). The length of the unit cell is therefore $17a_0$, i.e. 16 diffraction spots appear in between the integer spots along the $[\bar{1}\bar{1}2]$ direction.

Obviously for clean Si(557) the surface energy is minimized by the formation of (7×7) reconstructions on one half of the unit cell. The Si atoms of atomic steps from vicinal Si(111) surfaces with inclinations towards the $[\bar{1}\bar{1}2]$ direction have two unsaturated dangling bonds. These dimerize and explain the period doubling along the step edges. Recent high resolution STM experiments have shown that additional adatom structures on the mini (111) facets are present, stabilizing the triple step configuration of the Si(557) surface further [16].

3.2. Facet stabilization by a Pb monolayer

In this subsection, we show that the situation changes completely when coverages close to a physical monolayer Pb (1.2 ML with respect to the Si(111) surface density) are adsorbed on

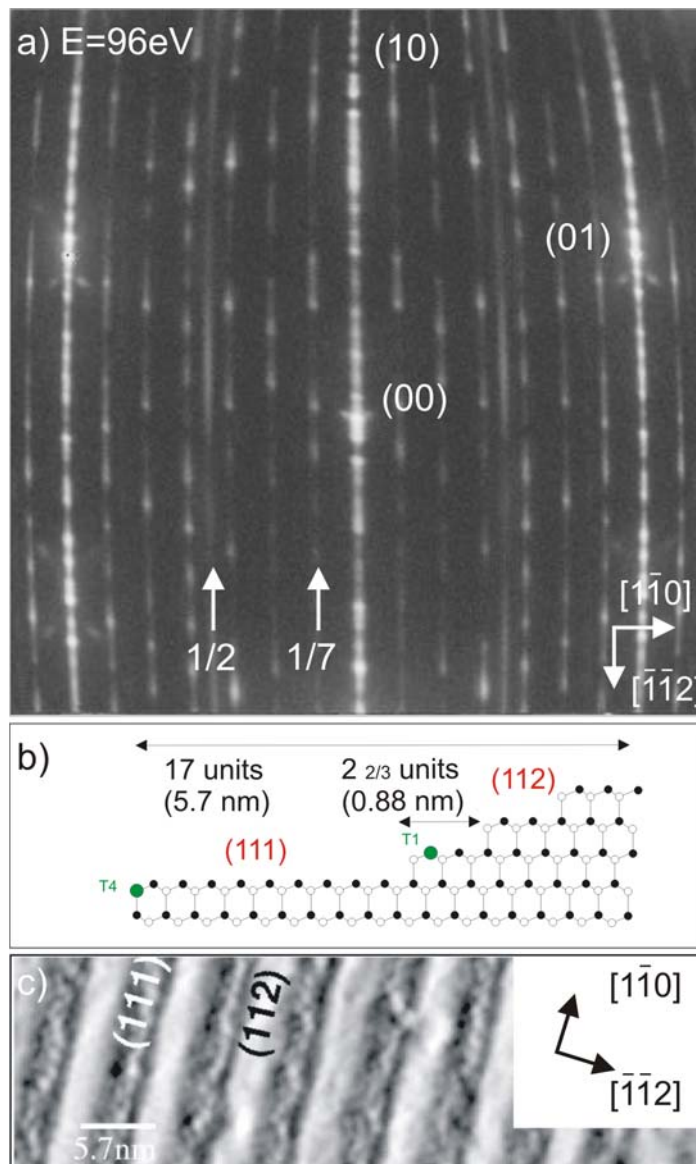


Figure 1. (a) Low energy electron diffraction (SPA-LEED) image of the clean Si(557) surface. (b) Sketch (side view) of the (557) unit cell. The clean Si(557) surface transforms into (111) and (112) facets. The alternating arrangements of these mini-facets are seen by STM shown in (c) ($T = 40$ K).

Si(557). As will be demonstrated, new terrace widths are stabilized and can even be modified by Pb concentration. We start with the most stable structure at 1.3 ML, and then demonstrate in the next subsection changes of step densities induced by small changes of Pb concentrations.

The diffraction pattern obtained after the deposition of 1.3 ML at $T = 80$ K followed by annealing to 600 K is shown in figure 2. Systematic annealing experiments have shown, that the (7×7) reconstruction is destroyed by annealing at 570 K (as judged by LEED). However, small partial units of (7×7) seem to remain, because an effective step mobility is only obtained for temperatures above 600 K [17]. Please note that once this destruction of (7×7) units is

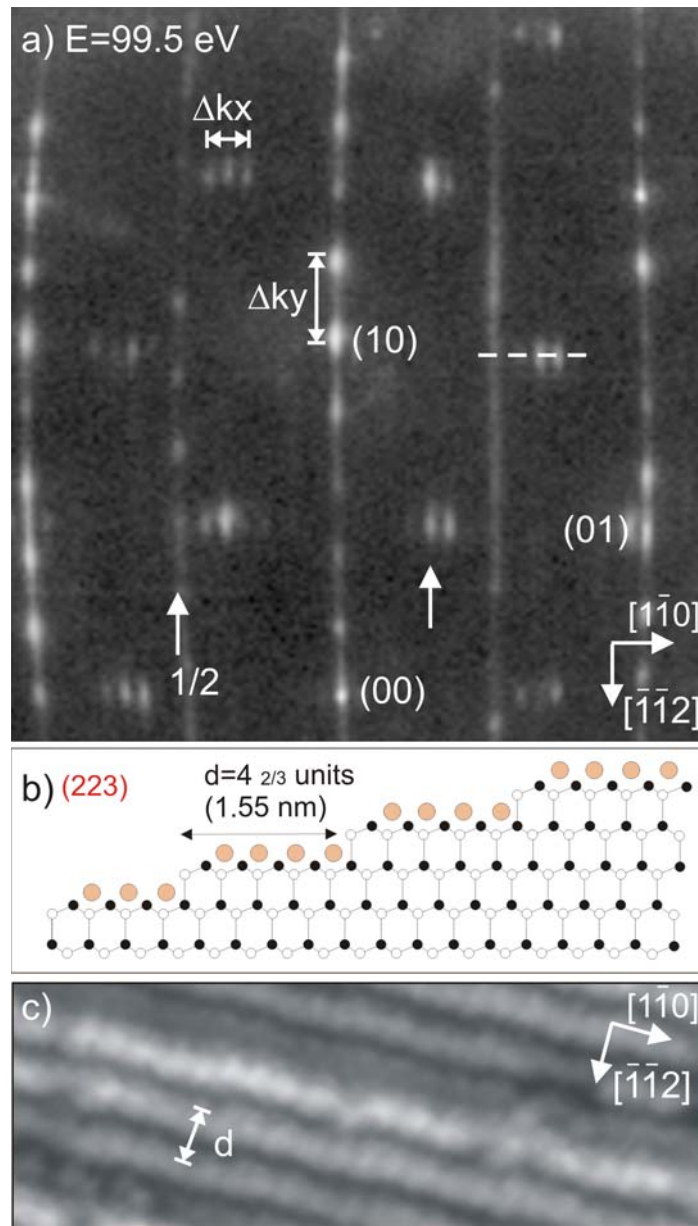


Figure 2. (a) LEED pattern after adsorption of 1.3 ML Pb and annealing to 600 K. The formation of an equally stepped surface with an average step–step distance of 1.55 nm results, as seen by the spot splitting of 21.3% SBZ, in agreement with STM (c) taken at $T = 40$ K. A schematic side view is shown in (b). The small circles denote Si atoms, the larger grey (orange) ones Pb atoms within the first monolayer.

complete, step mobilities can be observed at temperatures as low as 80 K (see below). In this first step, even better order is obtained when multilayers of Pb are first adsorbed and subsequently desorbed at 640 K leaving the same residual coverage on the surface, as explicitly checked by Auger spectroscopy for both preparation methods.

The most obvious change compared with the clean surface is the spot splitting along the $[\bar{1}\bar{1}2]$ direction. Only four spots appear in between (00) and (10) spots. The splitting of $k_y = 21.3\%$ SBZ (compared with 5.9% on the clean surface) corresponds to a periodically stepped surface with an average step distance of $4\frac{2}{3}a_0 (= 1.55 \text{ nm})$. This phase has been found recently with STM, too (see figure 2(c) [8]). In addition, the (7×7) reconstruction is not visible any longer in figure 2(a). Instead a new superstructure at the $\sqrt{3}$ positions appears, which shows a spot splitting of 10% SBZ in the $[1\bar{1}0]$ direction, i.e. along the terraces.

This result shows that a coverage of one physical monolayer of Pb is able to destabilize even the most stable (111) facet by modifying the surface energy. This is an activated process, since it occurs only by an annealing step close to the desorption temperature of Pb. The alternating (111) and (112) facets are now replaced by a homogeneously stepped surface. But, different from what is expected for repulsive step-step interactions, the resulting average terrace width does *not* correspond to that of the macroscopically cut (557) surface with an average terrace width of $5\frac{2}{3}a_0$. Instead, the initial step structure transforms into a (223) facet structure with an average terrace width of only $4\frac{2}{3}a_0$ as depicted in figure 2(b). These results are in agreement with recent ARPES investigations carried out by us [10], which reveal a nested Fermi surface.

The validity of the model and the quality of the new Pb stabilized (223) facet is directly demonstrated by the $(k_{\perp}, k_{\parallel})$ -plot shown in figure 3. For this graph, scans along the $[\bar{1}\bar{1}2]$ direction were taken at electron energies between 80 and 230 eV in steps of 1 eV and their intensities were mapped onto a grey scale coded image. The circles denote the Bragg-points of the Si(111) surface. The rods measured over five 3D Bragg conditions demonstrate the macroscopic rearrangement of the (557) surface into a (223) facet structure. The mismatch between the macroscopically oriented (557) surface and the (223) facets is compensated most likely by small facets with opposite inclination angles, e.g. (331) facets. Indications of them are seen within the transfer widths of the SPA-LEED instrument only by faint intensity streaks at some Bragg-points (see arrow in figure 3). Furthermore, also wider (111) terraces may be formed locally to maintain the macroscopic orientation of the sample. A remarkable feature in figure 3 is the uniform width of the rods, which means a small variance in the terrace size distribution [18]. The largest full widths at half maximum (FWHM) of these rods between the Bragg points is around 5% SBZ.

The possibility that the steps of the initial (557) surface are simply overgrown by Pb, forming a homogeneously stepped metallic surface on top, can be safely excluded for several reasons. Firstly, a much higher coverage than one physical monolayer would be needed, which is far outside the uncertainty of our coverage calibration. Secondly, since the size distribution is very narrow, a change of the step density by additional Pb requires the addition of a sequence of 1, 2, 3...Pb chains on subsequent terraces in order to change the step density on a larger scale. This arrangement cannot be stabilized for simple entropic reasons. It further requires the local formation of a second Pb layer, which would be unstable to high temperature annealing. Thirdly, the (2×1) reconstruction from the Si-step sites disappears by overgrowth at coverages above 1.4 ML (see below). Therefore the coverage must be smaller.

These results already demonstrate that the interface as a whole is transformed by a Pb monolayer into a regularly stepped surface with a step density different from the clean Si(557) surface. This is obviously the energetically favored configuration of this metal/semiconductor system.

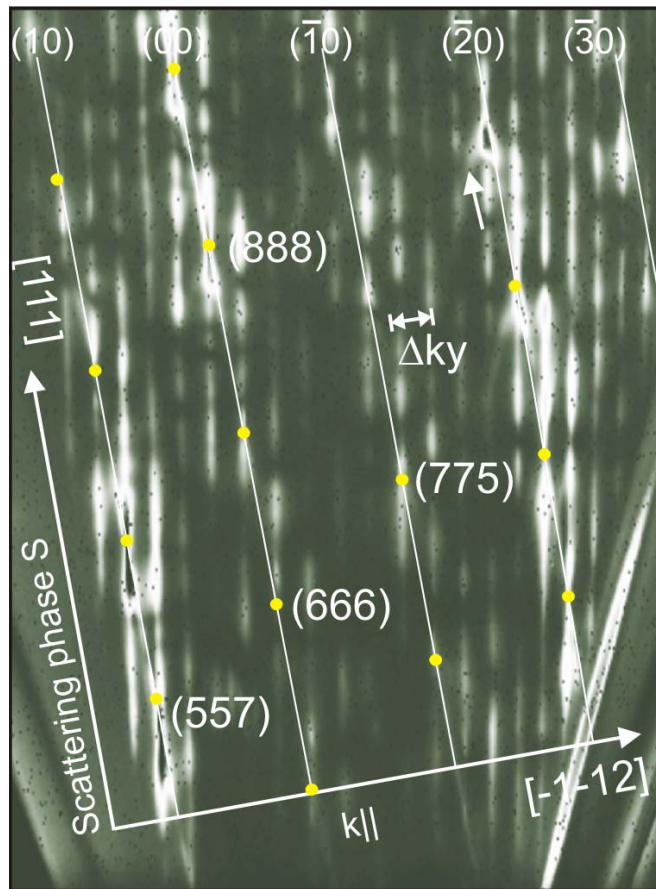


Figure 3. $(k_{\perp}, k_{\parallel})$ plot of 1.3 ML Pb on Si(557). Scans along the $[\bar{1}\bar{1}2]$ direction were taken for electron energies between 80 and 230 eV in steps of 1 eV. Their intensities are shown as a grey scale coded image (white means high intensity). The grey (yellow) circles mark the Bragg-points of the Si(111) surface for better orientation. The graph shows nicely the rods of the (223) facets.

3.3. Devil's staircase phases

Before we investigate changes of the surface morphology by varying Pb concentrations in the range between 1.2 and 1.3 ML, we will focus in the following on the lateral arrangement of Pb at coverages above 1.30 ML. As will be shown, they resemble closely the devil's staircase phases found on Pb/Si(111) [12]. In this range of coverage, the (223) orientation of facets remains unchanged.

The spot splitting of the superstructures seen in figure 2 can be explained by formation of so-called linear (m,n) -phases, a combination of $m\sqrt{7} \times \sqrt{3}$ and $n\sqrt{3} \times \sqrt{3}$ units, which appear in our case only as a single domain structure along the terraces. The combination of all possible (m,n) values forms a devil's staircase. A structural model of a (1,5) phase, which was most easily formed in our case, is shown in figure 4. According to the model outlined for the monolayer regime of Pb/Si(111) [12], the unit cell of the $\sqrt{3} \times \sqrt{3}$ phase consists of four Pb atoms (one on the centered H3 and three on off-centered T1 places), i.e. the coverage is $\frac{4}{3}$ ML, whereas the

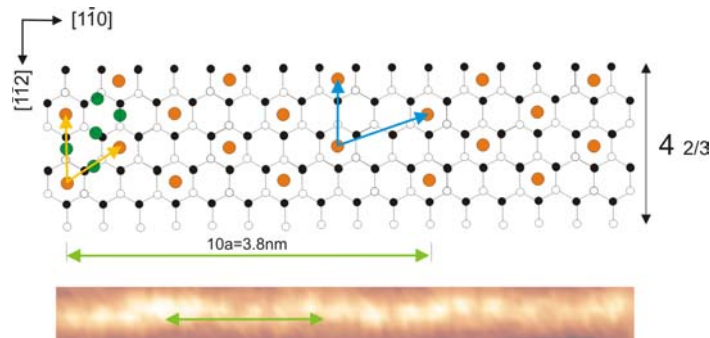


Figure 4. Model of the (1,5) phase of 1.31 ML Pb on Si(557). The closed and open small circles denote Si atoms of the first and second substrate layer, respectively. The light grey (orange) filled circles represent Pb atoms on H3 positions. The dark grey filled (green) circles are Pb atoms on off-centered T1 positions, exemplarily shown only for first $\sqrt{3} \times \sqrt{3}$ unit cell. This linear phase can be seen as a 10-fold periodicity within a single Pb-chain by STM [7].

($\sqrt{7} \times \sqrt{3}$) cell contains six Pb atoms (one on H3, five on off-centered T1) per five Si atoms. The coverage of a (1,5) phase is therefore 1.31 ML.

In diffraction experiments these linear phases are seen as spots appearing with different splitting around $\sqrt{3}$ -sites. The splitting of $k_x \approx 10\%$ SBZ corresponds to a 10-fold periodicity along the Pb-chain direction and is in good agreement with our STM results, which have revealed a modulation along the Pb chain. A magnification of such a modulated Pb chain is shown at the bottom of figure 4 [7]. It should be noted that the terraces of the (223) facets have sufficient width to form ordered $\sqrt{3}$ -units on these terraces. This is different for other facet orientations, as we will show below.

Proof that the (1,5) phase mentioned above is indeed part of a devil's staircase is shown in figure 5, where line scans through the (00) spot along the $[1\bar{1}0]$ direction, i.e. parallel to the step edges around the $\sqrt{3}$ -positions are shown. Varying the coverage by subsequent addition of small amounts of Pb between 1.30 and 1.314 ML at a surface temperature of 80 K (LEED measurements at 4 K), the splitting of the $\sqrt{3}$ spots changes from 14.2 to 8.1% SBZ. This corresponds to a change from a (1,3) to a (1,6) phase. Ordering of these phases requires some diffusion of Pb even at 80 K. Such low activation barriers are typical and have been reported also for the Pb/Si(111) system within the devil's staircase coverage regime [12]. The accompanied ultra-fast kinetics of these phases have been discussed recently in terms of a collective diffusion coefficient with singularities at distinct coverages, i.e. at the devil's staircase phases [19]. In fact, the phases ranging from (1,3) to (1,6) have been used to calibrate the Pb coverage most precisely.

For a Pb coverage of 1.42 ML the splitting is around 8% SBZ and remains constant up to 1.62 ML. This phase is comparable to a stripe-incommensurate (SIC) phase, seen for Pb/Si(111) at coverages higher than 1.34 ML [19]. The periodicity of this SIC phase is $(12 \times \sqrt{3})$, slightly smaller than the $(13 \times \sqrt{3})$ and $(14 \times \sqrt{3})$ structures suggested in [20, 21] for Pb on Si(111). This small difference may be due to an influence of the steps on ultra-short (111) terraces. It should also be mentioned that in contrast to the Pb/Si(111) system, the linear phases and the SIC-structures can be distinguished only by the spot splitting of the superstructures along the $[1\bar{1}0]$ direction.

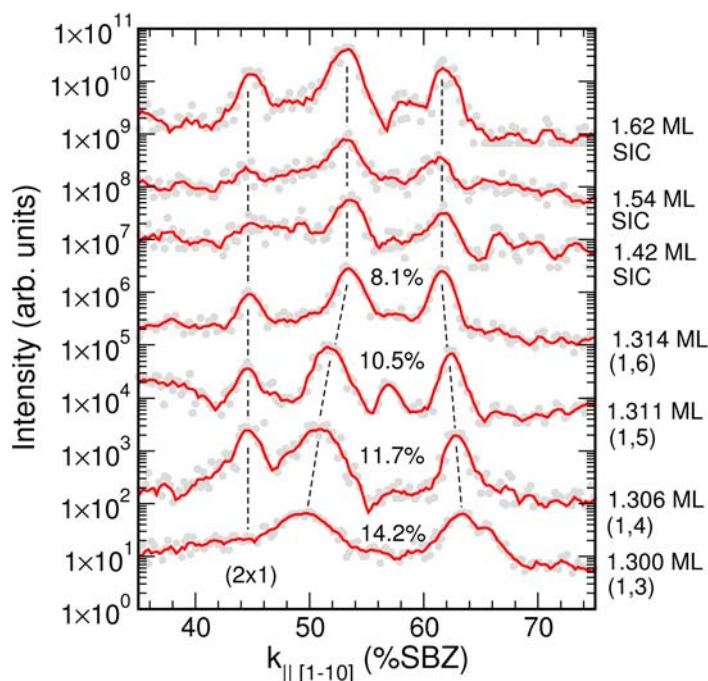


Figure 5. Line scans taken along the $[1\bar{1}0]$ direction at $E = 99.5$ eV ($S = 5.1$). Shown is the region around the $\sqrt{3}$ positions (cf with dashed line in figure 2(a)). The gradually shrinking spot splitting with increasing coverage is the signature for different linear phases (m,n) . For coverages between 1.4 and 1.6 ML the SIC phase is found with a constant spot splitting of 8% SBZ (solid curve = 5-pt averaging).

In the LEED pattern of figure 2 at a Pb coverage of 1.30 ML the streaks at half order positions of the clean (557) surface have developed into clear spots with a separation again of 21.3% SBZ, i.e. the separation of the steps at this Pb concentration. This not only shows that the dimerization at the step edges still survives after Pb adsorption of 1.30 ML, there must also be a strong correlation between the step edges. Otherwise the spot would again appear as streaks along the $[\bar{1}\bar{1}2]$ direction.

This (2×1) reconstruction along the step edges shows a characteristic coverage dependence. It disappears for coverages between 1.4 and 1.5 ML, which indicates a step decoration by excess Pb atoms. For higher coverages, the (2×1) intensity appears again, i.e. after completion of the decoration process. Obviously, Pb first covers the terraces, then fills the step sites at coverages around 1.4 ML, but leaves the dimerization of the Si step structure unchanged once all step sites are filled by Pb.

3.4. Coverage-dependent step trains

In this subsection, we show that, unlike the situation for the physical monolayer coverage and above ($\Theta > 1.33$), where the (223) facet structure is conserved, the average step separation becomes unstable at smaller Pb concentrations between 1.2 and 1.3 ML. As a consequence, other inclinations of the initial (557) surface are found.

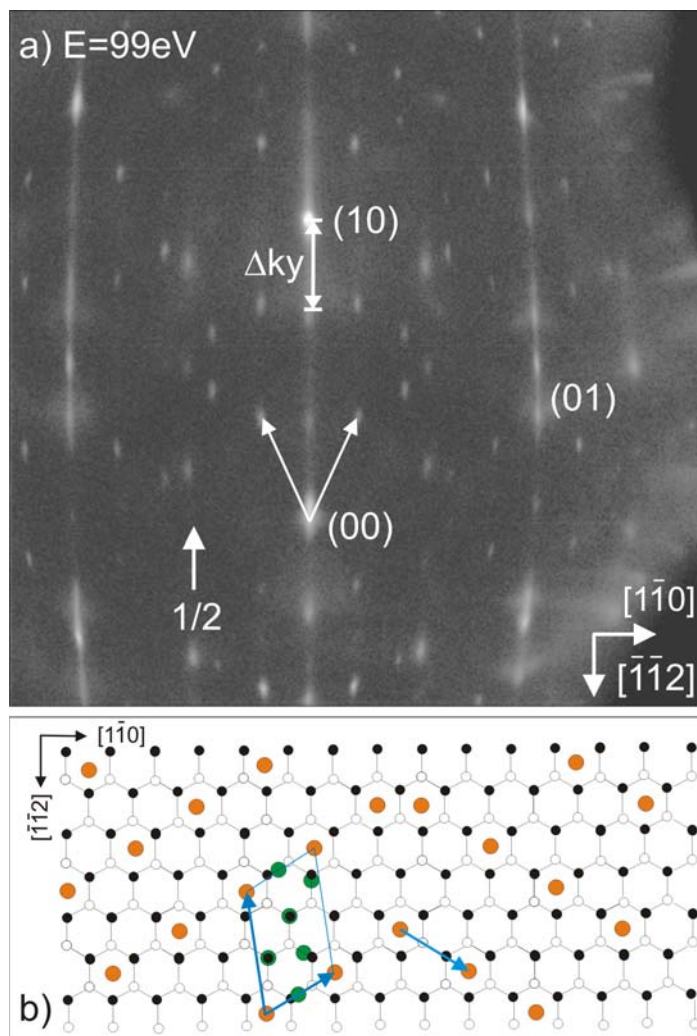


Figure 6. (a) LEED pattern obtained for 1.22 ML Pb/Si(557) ($T = 40$ K). (b) Shows the mirror domain ($\sqrt{7} \times \sqrt{3}$) structure on (111) terraces. Larger grey (orange) circles denote Pb atoms on the H3 positions. The dark grey (green) larger circles are Pb atoms adsorbed at off-centered T1 sites. The only superstructures from the (112) facets are the half order spots.

The pattern shown in figure 6 was obtained by partial desorption of Pb at a surface temperature of 640 K, starting from, e.g., 1.3 ML coverage. The remaining Pb coverage is 1.20 ML as judged from the two domains of pure $\sqrt{7} \times \sqrt{3}$ LEED structure seen in this figure. Since the spots are not elongated, this structure must be formed on portions of the surface with large (111) terraces. The same structure can also be obtained by adding Pb to a lower coverage after the high temperature annealing step has taken place.

In addition, the step structure, visible from the spot splitting of integer order spots, has significantly changed compared with the 1.3 ML phase, although the difference in Pb coverage is only 0.1 ML. The separation of $k_y = 37.3\%$ SBZ belongs to a step train of (112) facets, with (111) terraces that are only $2\frac{2}{3}a_0$ wide. These facets are too small to allow formation of a

$(\sqrt{7} \times \sqrt{3})$ superstructure. It can only form on larger (111) terraces, which compensate for the high inclination of the (112) facets. As depicted in figure 6(b), a $(\sqrt{7} \times \sqrt{3})$ mirror domain structure can be formed on these larger terraces, in perfect agreement with the LEED pattern. All atoms of Pb in this phase are shown exemplarily only in one of the unit cells. Due to the vicinity of the surface, the third domain is missing, i.e. only faint intensity features are seen sometimes.

According to the LEED and STM investigations for Pb/Si(111) [12], the coverage of this $(\sqrt{7} \times \sqrt{3})$ structure is 1.20 ML. Again, and similar to the (1,5) linear phase of figure 2(a), the half order spots for this Pb coverage have the same spot splitting as the integer spots. This supports the assumption from above that this reconstruction stems indeed from the step sites of the surface.

Together with changes in the lateral structures on the (111) terraces as a function of Pb concentration, the step train structure can be further tuned from (112), (335) to (223) facets and finally even to steps trains, which correspond to equally stepped (557) substrates, by increasing the Pb concentration gradually between 1.20 and 1.35 ML. The homogeneously stepped (557) orientation with 18% SBZ spot splitting is the least stable of these phases and is visible only for adsorption temperatures below 80 K and a coverage around 1.34 ± 0.02 ML. At higher temperatures it transforms back to the (223) facets described above.

This sequence (apart from the homogeneously stepped (557) surface) was found in evaporation experiments at a surface temperature of 180 K, in which small concentrations of Pb were added. After evaporation, the samples were always cooled to 4 K for the LEED observations. Figure 7 shows a sequence of line scans taken across the step direction for coverages ranging from 1.2 ML to 1.62 ML. The addition of 0.04 ML to the 1.2 ML shown in figure 5 results in a (4,1) linear phase structure (again on larger (111) terraces). The spot splitting in the direction normal to the steps is $k_y = 27.3\%$ SBZ, characteristic of a (335) facet orientation. The high mismatch between these phases and the original (557) inclination is manifested by the high FWHM value, which is larger than 10% SBZ. Finally, further adsorption of 0.06 ML leads to the formation of the already known (223) facet orientation. The 21.3% SBZ splitting is clearly visible and remains visible for coverages up to 1.62 ML.

We emphasize here that the morphological changes resulting from the variation of the step density in presence of a monolayer of Pb are already possible at deposition temperatures as low as 180 K (and in the case of (557) even around 80 K!). This shows that monolayer adsorption of Pb has strongly weakened the Si bonds particularly at step edges so that Pb–Si complexes can diffuse effectively and rearrange the step structure already at these low temperatures. There is still an activation barrier, however, since better ordering is obtained after annealing to 600 K, slightly below the desorption threshold.

From the profile in figure 7 taken at 1.42 ML coverage, it seems that the step train can also be modified at Pb coverages higher than one physical monolayer. The addition of 0.1 ML of Pb at 180 K to the linear phases with a coverage around 1.32 ML, e.g. (1,5), results in period doubling along the $[\bar{1}\bar{1}2]$ direction, whereas the splitting along the $[1\bar{1}0]$ remains at 8% SBZ (cf with figure 6). Adding once more 0.1 ML of Pb results in complete removal of this periodicity doubling, and the well known 21.3% SBZ splitting of the (223) reappears.

Therefore, morphological changes of the step train are unlikely in this case. In fact, this finding is fully compatible with the assumption already made above that up to a coverage of 1.32 ML the step edges are not covered by Pb. The addition of approximately 0.1 ML of Pb suffices to decorate every second step. It corresponds well with the average step density of

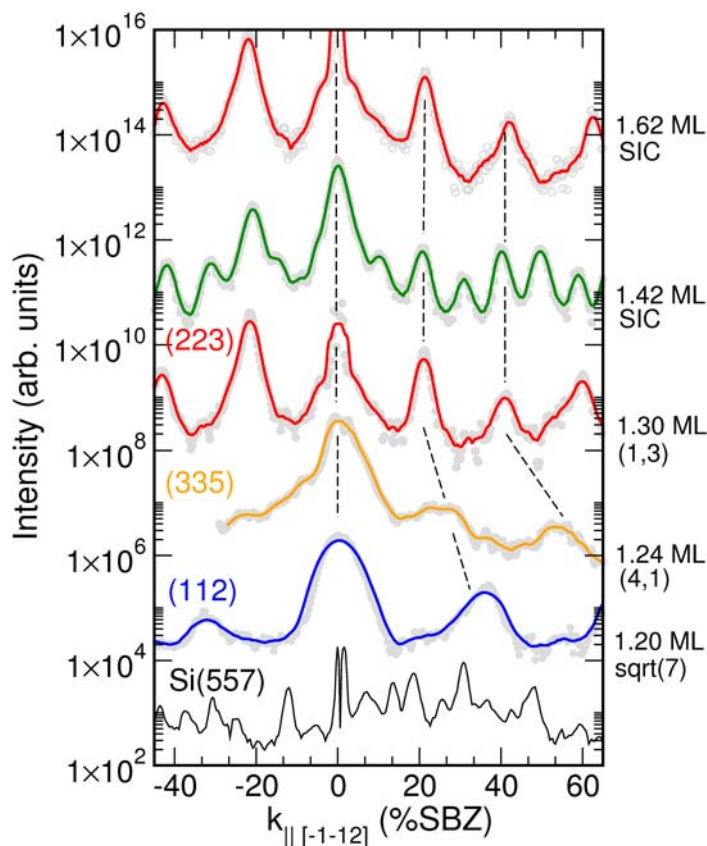


Figure 7. (a) Line scans along the $[\bar{1}\bar{1}2]$ direction for coverages between 1.20 and 1.62 ML. The deposition was carried out at 180 K, whereas the measurement was done at 4 K at an electron energy of 99.5 eV.

$2 \times 4\frac{2}{3}$ unit cells. The second addition of the same amount of Pb fills all step edges, and the original periodicity reappears.

4. Discussion

Our results show that Pb coverages in the monolayer regime between 1.2 and 1.3 ML are able to destabilize the macroscopically cut vicinal Si(557) surface and to readjust the step density depending on Pb coverage. This happens already at temperatures below 180 K, and for a small range of concentration even at 80 K once the Si(7×7) order is removed. Fairly high diffusion coefficients are necessary even at these low temperatures, which at first glance seems to be surprising. However, as shown recently by Yakes *et al* [22] for the monolayer regime of Pb/Si(111), at which the devil's staircase phases appear, temperatures as low as 40 K suffice to make Pb mobile, with typical singularities in the (calculated) diffusion coefficients at the completion of ordered phases. While these results are not directly transferable to our system, where the diffusion of both Pb and Si atoms is necessary, they show that low activation energies for diffusion are involved in the Pb/Si system, especially at critical concentrations that lead to structural changes.

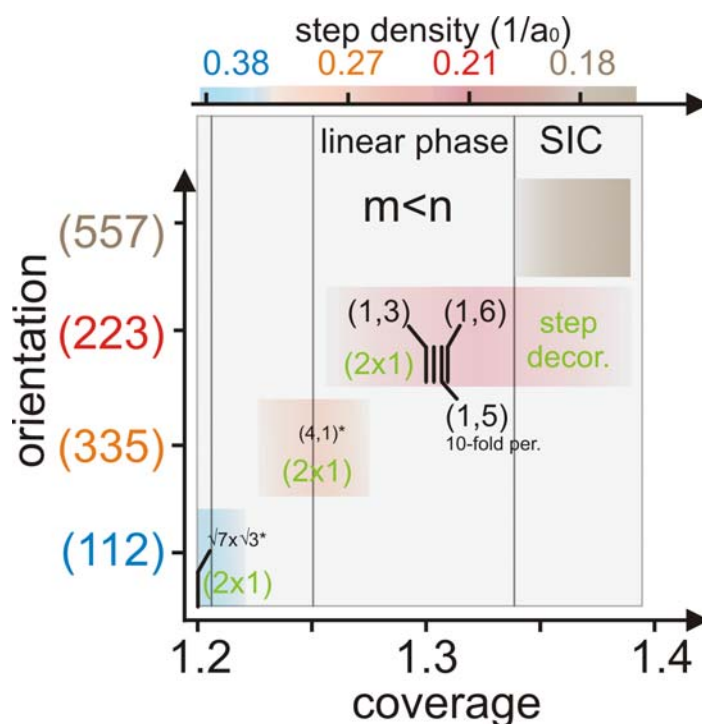


Figure 8. Phase diagram for Pb/Si(557). The (*) marked phases appear only on larger (111) terraces. For further details see text.

The steps in this system play a particularly important role, since their density changes dramatically with Pb concentration. Contrary to what might be expected, the steps themselves cannot act as nucleation sites on these stepped surfaces, since the periodic step train structure, irrespective of the orientation of the facets, always maintains the (2×1) reconstruction that already exists for the clean (557) surface. That the Si dimers of the clean surface are not replaced by, e.g. Pb-dimers is consistent with STM results for Pb/Si(100) [23]. These results show that the Pb–Si bond on the dimerized surface is so weak that it is not able to lift Si–Si dimerization. Therefore, it seems reasonable to assume that Pb covers predominantly only the small (111) terraces without occupying the step edges.

We can go even one step further: local monolayer formation ($\Theta = 1.33$ ML) on small terraces seems to be the most stable configuration on these stepped surfaces, even at the expense of creating additional step edges. This seems to be the case for a coverage of 1.2 ML, at which (112) facets are formed with an extremely high step density. Following this argument as a function of increasing Pb concentration, additional Pb should be adsorbed on (111) terrace sites, not on step edges. This can only be managed by increasing the terrace widths, thereby reducing the step density.

Indeed, this model works almost quantitatively, as figure 8 shows. Here, we plotted the ranges of stability of the various facets as a function of Pb concentration (bottom axis) and simultaneously as a function of decreasing step density. The decreasing step density corresponds well to the increment of Pb concentration starting at 1.2 ML and corroborates our model. Thus, the driving force for the facetting is the Pb adsorption energy that depends strongly on local configuration and coordination. It is interesting to note that the (223) facet in presence of Pb

turns out to be the most stable configuration that finally survives. Only at higher concentrations, where second Pb layer formation starts, can steps also be decorated on these most stable (223) facets.

The electronic consequences have so far been only explored for the (223) facet orientation. As known for other systems, e.g. Ag and Au adsorbed on Si(111) [24, 25], the stability of surface phases depends strongly on the filling factors of the surface band structure, i.e. on the coverage of the adatoms. For these (223)-facets, with a terrace width of $4\frac{2}{3}a_0$ we found indeed [10], that the Fermi wavevector k_F is half a reciprocal lattice vector $g = 2\pi/d$ with $d = 4\frac{2}{3}a_0$, which results in Fermi nesting and in gap opening. Thus, there may also be an electronic contribution to the stabilization of this structure, whereas any step–step interaction does not play an important role.

5. Summary

We have shown in this SPA-LEED analysis that adsorption of Pb in the monolayer regime on vicinal Si(111) leads to the formation of several uniformly faceted surfaces. Generally, the equilibrium structure of vicinal surfaces is determined by both the terraces and the steps. With adsorbed Pb, the differences in surface energies between terraces and steps are strongly enhanced in the monolayer regime.

Depending on the exact coverage, different Pb-phases as well as different step–step distances, i.e. (112), (335), (223) and (557) orientations, have been found. Furthermore, the lateral Pb–phase *and* the vicinality can be tuned gradually and reversibly by changing the Pb coverage. Whereas for $T = 80$ K only terrace diffusion is effective, the Ehrlich–Schwoebel barrier between the terraces is overcome for substrate temperatures already below 180 K.

Parts of devil’s staircase phases can only develop on the larger (223) terraces close to 1.3 ML.

Because of the strong sensitivity of the Pb adsorption energy to local coordination, the main mechanism for stabilization of the facets by monolayers of Pb seems to be the avoidance of step occupation. Therefore the step density is adjusted so that all Pb atoms can be adsorbed on (111) oriented terrace sites.

References

- [1] Dil J H, Kampen T U, Hülsen B, Seyller T and Horn K 2007 *Phys. Rev. B* **75** 161401
- [2] Yeh V, Berbil-Bautista L, Wang C Z, Ho K M and Tringides M C 2000 *Phys. Rev. Lett.* **85** 5158
- [3] Vilfan I and Pfnür H 2003 *Eur. Phys. J. B* **36** 2817
- [4] Yeom H W *et al* 1999 *Phys. Rev. Lett.* **82** 4898
- [5] Crain J N, Kirakosian A, Altmann K N, Bromberger C, Erwin S C, McChesney J L, Lin J-L and Himpsel F J 2003 *Phys. Rev. Lett.* **90** 176805
- [6] Crain J N and Himpsel F J 2006 *Appl. Phys. A* **82** 431
- [7] Tegenkamp C and Pfnür H 2007 *Surf. Sci.* **601** 2641
- [8] Tegenkamp C, Kallassy Z, Guenter H-L, Zielasek V and Pfnür H 2005 *Eur. Phys. J. B* **43** 557
- [9] Tegenkamp C, Kallassy Z, Pfnür H, Günter H-L, Zielasek V and Henzler M 2005 *Phys. Rev. Lett.* **95** 176804
- [10] Tegenkamp C, Ohta T, McChesney J L, Pfnür H and Horn K submitted
- [11] Kim K S, Choi H and Yeom H W 2007 *Phys. Rev. B* **75** 195324
- [12] Yakes M, Yeh V, Hupalo M and Tringides M C 2004 *Phys. Rev. B* **69** 224103

- [13] Stepanovsky S, Yakes M, Yeh V, Hupalo M and Tringides M C 2006 *Surf. Sci.* **600** 1417
- [14] Kirakosian A, Bennewitz R, Crain J N, Fauster Th, Lin J-L, Petrovykh D Y and Himpsel F J 2001 *Appl. Phys. Lett.* **79** 1608
- [15] Phaneuf R J and Williams E D 1990 *Phys. Rev. B* **41** 2991
- [16] Tey S A, Romanyuk K N, Zhachuk R A and Olshanetsky B Z 2006 *Surf. Sci.* **600** 4878
- [17] Schuster A, Czubanowski M, Pfnür H and Tegenkamp C to be published
- [18] Tong X and Bennett P A 1991 *Phys. Rev. Lett.* **67** 101
Tegenkamp C *et al* 2002 *Phys. Rev. B* **65** 235316
- [19] Yakes M, Hupalo M, Zaluska-Kotur M A, Gortel Z W and Tringides M C 2007 *Phys. Rev. Lett.* **98** 135504
- [20] Choi W H, Koh H, Rotenberg E and Yeom H W 2007 *Phys. Rev. B* **75** 075329
- [21] Hoque E, Petkova A and Henzler M 2002 *Surf. Sci.* **515** 312
- [22] Yakes M, Hupalo M, Zaluska-Kotur M A, Gortel Z W and Tringides M C 2007 *Phys. Rev. Lett.* **98** 135504
- [23] Dong Z-C, Fujita D and Nejoh H 2001 *Phys. Rev. B* **63** 115402
- [24] Crain J N, Altmann K N, Bromberger C and Himpsel F J 2002 *Phys. Rev. B* **66** 205302
- [25] Crain J N, Gallagher M C, McChesney J L, Bissen M and Himpsel F J 2005 *Phys. Rev. B* **72** 045312